

Supplemental: Climatology of aerosol properties at an atmospheric monitoring site on the Northern California coast

Erin K. Boedicker¹, Elisabeth Andrews¹, Patrick J. Sheridan², Patricia K. Quinn³

¹Cooperative Institute for Research in Environmental Sciences (CIRES), University of Colorado, Boulder, Colorado

²Global Monitoring Laboratory, National Oceanic and Atmospheric Administration, Boulder, Colorado

³Pacific Marine Environmental Laboratory (PMEL), National Oceanic and Atmospheric Administration, Seattle, Washington

Correspondence to: Erin K. Boedicker (erin.boedicker@noaa.gov)

Number of pages: 21

Number of figures: 13

Number of tables: 12

CONTENTS

Section S1: Measurement Comparisons to DRUM data

Section S2: Meteorology at THD

Section S3: Aerosol composition climatology and results of linear regression analysis for ion data

Section S4: Further details of PMF and error analysis

Section S5: Detailed seasonal and diurnal trends for $f(\text{RH}=85\%)$

Section S6: Aerosol type classification as a function of season and wind direction

Section S7: Aerosol ion and optical properties comparison information

Section S1: Measurement Comparisons to DRUM data

Data in this section refers to samples collected during the ITCT 2K2 campaign by an eight-stage rotating drum impactor with the following aerodynamic diameter ranges: 10.0–5.0, 5.0–2.5, 2.5–1.15, 1.15–0.75, 0.75–0.56, 0.56–0.34, 0.34–0.24, and 0.24–0.09 mm. Samples were then analyzed using synchrotron X-ray fluorescence (SXRF) for elemental composition. Further details of this data can be found in Perry et al. (2004). The elemental masses for PM_{10} were calculated from this data and compared to the sample measurements presented within this paper in order to ensure that the two sampling methods were in relative agreement.

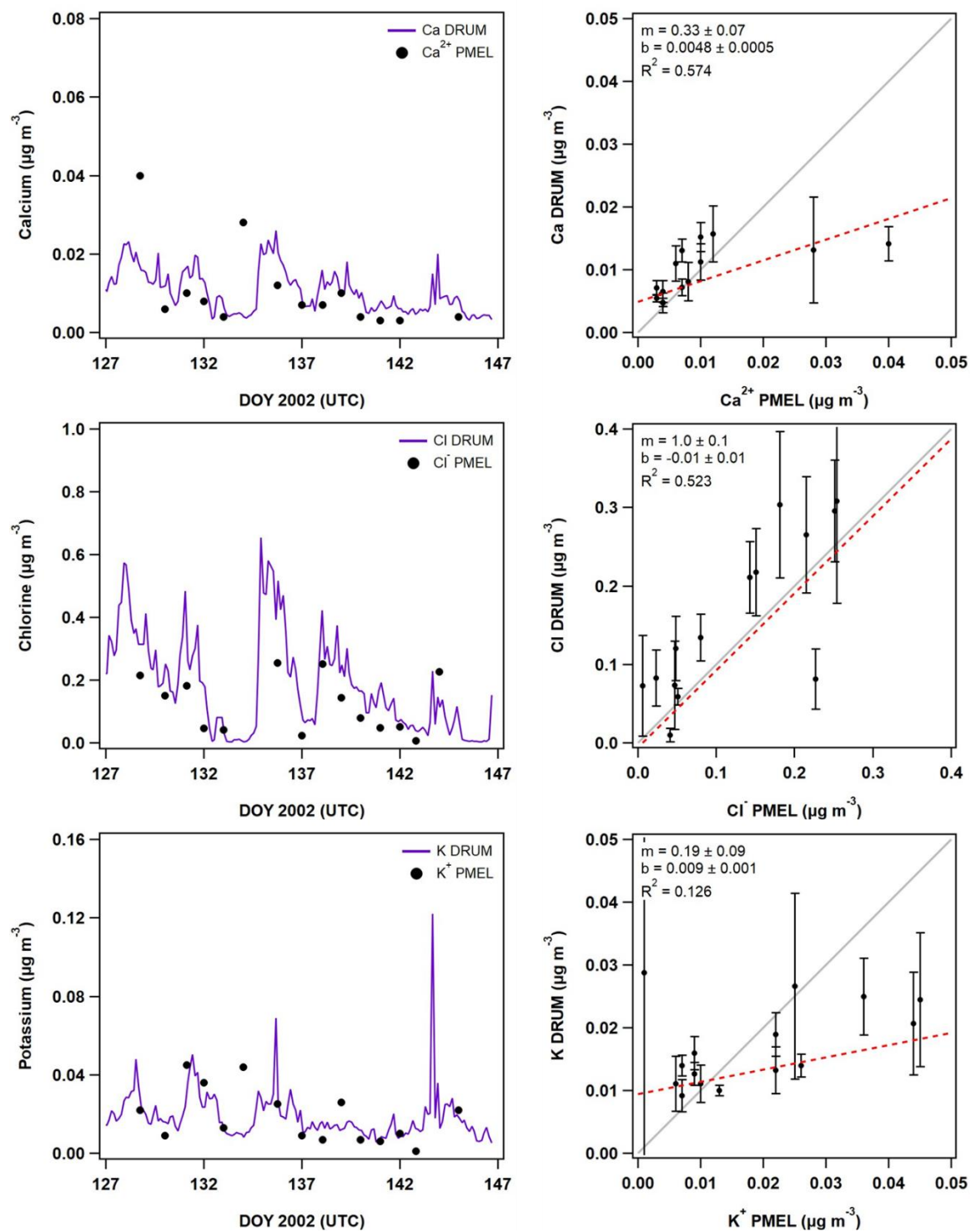


Figure S1: Comparison of the PMEL ion concentration data to the DRUM elemental composition measurements available from the Spring of 2002. Here the timeseries and linear regression comparisons are presented for Ca^{2+} , Cl^- , and K^+ .

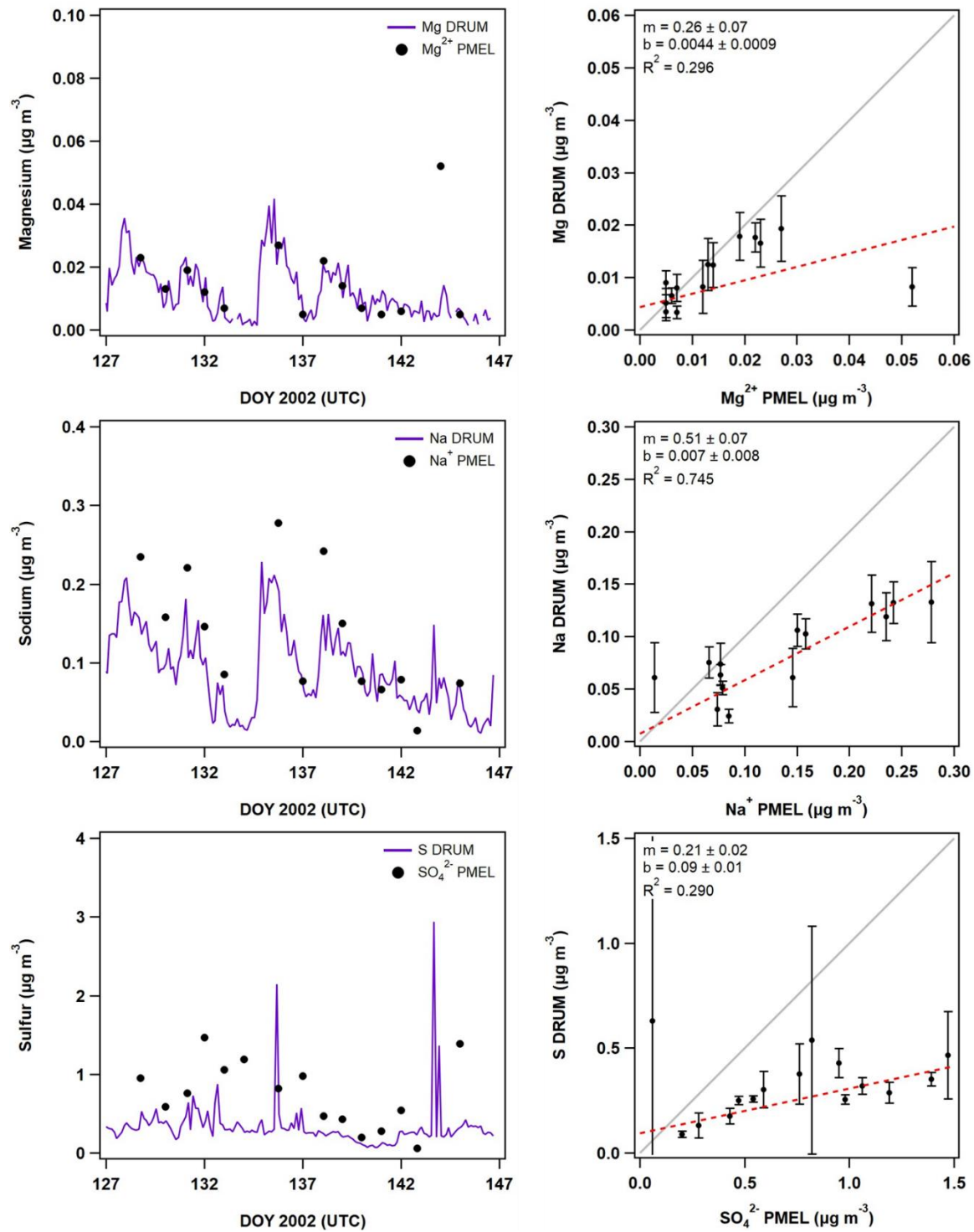


Figure S2: Comparison of the PMEL ion concentration data to the DRUM elemental composition measurements available from the Spring of 2002. Here the timeseries and linear regression comparisons are presented for Mg^{2+} , Na^+ , and SO_4^{2-} .

Section S2: Meteorology at THD

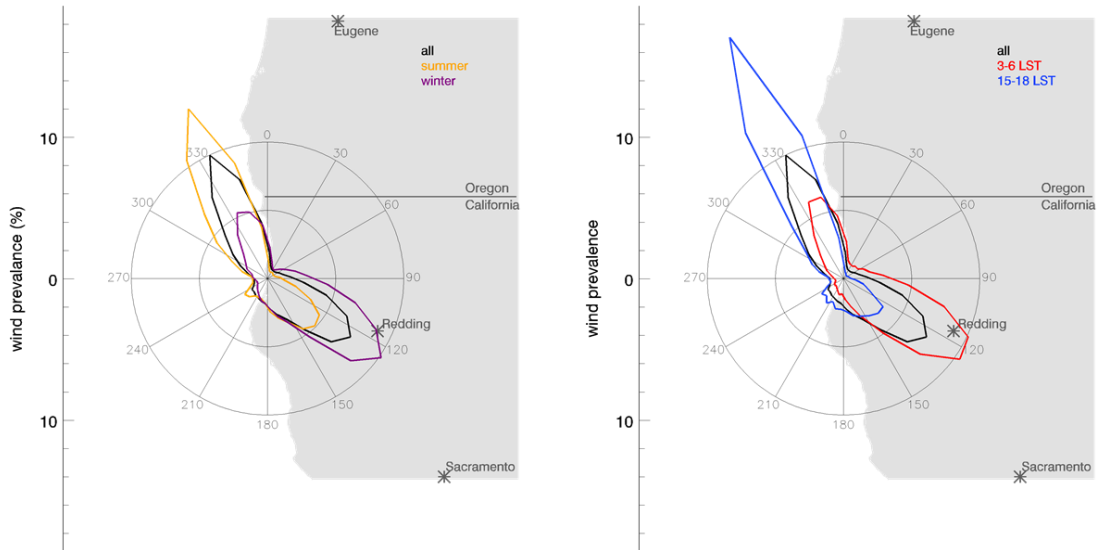


Figure S3: Map of Trinidad head sampling site and wind roses of prevalent wind directions. In the left panel the prevalent wind directions for all data are shown, as well as wind directions segregated by summer (June/July/August) and winter (December/January/February) months. In the right panel prevalent wind direction for all data are compared to times when a sea breeze (3-6 pm local time) or land breeze (3-6 am local time) may have been present due to thermally induced flow.

Section S3: Aerosol composition climatology and results of linear regression analysis for ion data

Table S1: Total and ion PM1 mass fraction of ion components for the four major seasons (winter, summer, spring, and fall). The total mass fractions were based on the ion concentrations relative to the PM1 mass while the ion mass fractions were based on the ion concentrations relative to the summed ion mass. The PM1 ion mass fraction data used to make **Figure 3** is bolded.

	Winter		Spring		Summer		Fall	
	Total %	Ion %	Total %	Ion %	Total %	Ion %	Total %	Ion %
SO ₄ ²⁻	4.4 ± 0.7	25 ± 6	13 ± 5	47 ± 10	21.8 ± 0.9	61 ± 1	11 ± 7	42 ± 6
NH ₄ ⁺	0.79 ± 0.07	4.4 ± 0.3	2.9 ± 0.9	11 ± 3	6.0 ± 0.5	16.6 ± 0.5	2 ± 2	10 ± 4
Cl ⁻	5 ± 1	28 ± 4	4 ± 2	14 ± 8	1.4 ± 0.2	3.9 ± 0.5	3 ± 2	20 ± 10
Br ⁻	0.02 ± 0.01	0.13 ± 0.05	0.02 ± 0.01	0.06 ± 0.04	0.04 ± 0.03	0.12 ± 0.07	0.026 ± 0.03	0.09 ± 0.04
Na ⁺	4.4 ± 0.7	25 ± 4	4 ± 1	16 ± 7	2.0 ± 0.3	5.7 ± 0.8	4 ± 1	17 ± 9
K ⁺	0.8 ± 0.2	4.3 ± 0.5	0.6 ± 0.2	2.4 ± 0.8	0.42 ± 0.07	1.2 ± 0.2	0.8 ± 0.2	3 ± 1
Ca ²⁺	0.5 ± 0.2	2 ± 1	0.3 ± 0.1	1.4 ± 0.6	0.15 ± 0.03	0.4 ± 0.1	0.26 ± 0.02	1.1 ± 0.3
Mg ²⁺	0.38 ± 0.06	2.1 ± 0.3	0.39 ± 0.07	1.5 ± 0.4	0.23 ± 0.03	0.66 ± 0.09	0.4 ± 0.1	1.7 ± 0.8
NO ₃ ⁻	0.93 ± 0.09	5.2 ± 0.2	0.6 ± 0.1	2.2 ± 0.7	0.36 ± 0.03	1.0 ± 0.1	0.66 ± 0.05	2.9 ± 0.6
MSA ⁻	0.14 ± 0.04	0.8 ± 0.2	0.7 ± 0.6	3 ± 2	2.7 ± 0.6	7 ± 1	0.8 ± 0.7	3 ± 2
Oxalate	0.6 ± 0.1	3.1 ± 0.3	0.66 ± 0.09	2.50 ± 0.08	0.64 ± 0.04	1.8 ± 0.2	0.8 ± 0.1	3.4 ± 0.4
Unknown	82 ± 2	-	73 ± 3	-	64 ± 2	-	76 ± 6	-
eBC*	2 ± 1	-	1.4 ± 0.3	-	0.97 ± 0.08	-	2.5 ± 0.5	-
Unknown	80 ± 2	-	72 ± 3	-	63 ± 2	-	74 ± 6	-

*Calculated from measured aerosol absorption coefficient and assume mass absorption coefficient (MAC) of XX m²/g

Table S2: Total and ion PM10 mass fraction of ion components for the four major seasons (winter, summer, spring, and fall). The total mass fractions were based on the ion concentrations relative to the PM1 mass while the ion mass fractions were based on the ion concentrations relative to the summed ion mass. The PM10 ion mass fraction data used to make **Figure 3** is bolded.

	Winter		Spring		Summer		Fall	
	Total %	Ion %	Total %	Ion %	Total %	Ion %	Total %	Ion %
SO ₄ ²⁻	2 ± 1	9 ± 1	5 ± 2	15 ± 4	6 ± 2	20 ± 2	4 ± 2	13 ± 5
NH ₄ ⁺	0.2 ± 0.2	0.6 ± 0.4	0.7 ± 0.5	2 ± 1	1.1 ± 0.4	3.5 ± 0.9	0.5 ± 0.4	2 ± 1
Cl ⁻	12 ± 5	48 ± 4	14 ± 1	41 ± 6	10.9 ± 0.3	35 ± 3	14 ± 2	44 ± 7
Br ⁻	0.03 ± 0.01	0.12 ± 0.02	0.03 ± 0.01	0.09 ± 0.01	0.03 ± 0.01	0.09 ± 0.02	0.04 ± 0.01	0.13 ± 0.03
Na ⁺	8 ± 4	31.6 ± 0.9	10 ± 2	30 ± 3	8.3 ± 0.8	26 ± 0.5	9.1 ± 0.8	29 ± 2
K ⁺	0.4 ± 0.2	1.47 ± 0.04	0.5 ± 0.1	1.4 ± 0.1	0.43 ± 0.07	1.36 ± 0.06	0.48 ± 0.03	1.51 ± 0.02
Ca ²⁺	0.3 ± 0.1	1.08 ± 0.04	0.4 ± 0.1	1.1 ± 0.3	0.25 ± 0.04	0.78 ± 0.08	0.29 ± 0.01	0.93 ± 0.07
Mg ²⁺	0.9 ± 0.4	3.4 ± 0.2	1.1 ± 0.2	3.2 ± 0.2	1.01 ± 0.03	3.2 ± 0.3	1.0 ± 0.1	3.1 ± 0.3
NO ₃ ⁻	1.1 ± 0.9	4 ± 2	1.9 ± 0.8	5 ± 2	2.2 ± 0.5	7 ± 2	1.9 ± 0.6	6 ± 2
MSA ⁻	0.05 ± 0.03	0.16 ± 0.08	0.2 ± 0.2	0.7 ± 0.4	0.7 ± 0.3	2.2 ± 0.6	0.2 ± 0.2	0.6 ± 0.6
Oxalate	0.08 ± 0.04	0.32 ± 0.06	0.2 ± 0.1	0.6 ± 0.2	0.25 ± 0.07	0.8 ± 0.2	0.21 ± 0.08	0.6 ± 0.2
Unknown	70 ± 10	-	65 ± 6	-	68 ± 3	-	68 ± 2	-
eBC*	0.20 ± 0.07	-	0.22 ± 0.04	-	0.16 ± 0.04	-	0.39 ± 0.06	-
Unknown	70 ± 10	-	65 ± 6	-	68 ± 3	-	68 ± 2	-

*Calculated from measured aerosol absorption coefficient and assume mass absorption coefficient (MAC) of XX m²/g

Table S3: Compilation of correlation coefficient (r) values for the PM1 relationships between different ion components in each season. The ion that was used on the y-axis is listed as the row and the ion it was plotted against on the x-axis is the column header. Fits that are not considered significant ($r < 0.5$) are listed in grey, highly significant fits ($r > 0.8$) are bolded.

		SO ₄ ²⁻	NH ₄ ⁺	Cl ⁻	Br ⁻	Na ⁺	K ⁺	Ca ²⁺	Mg ²⁺	NO ₃ ⁻	MSA ⁻	Oxalate
PM ₁	Winter	0.840	0.710	0.847	0.383	0.906	0.854	0.996	0.900	0.998	0.655	0.784
	Spring	0.595	0.618	0.350	0.700	0.518	0.612	0.613	0.510	0.570	0.230	0.784
	Summer	0.886	0.858	0.706	0.578	0.796	0.291	0.842	0.806	0.662	0.921	0.928
	Fall	0.753	0.564	0.560	0.122	0.694	0.915	0.540	0.675	0.806	0.473	0.943
SO ₄ ²⁻	Winter	-	0.945	0.522	0.092	0.687	0.739	0.622	0.691	0.431	0.793	0.779
	Spring	-	0.942	0.266	0.693	0.400	0.741	0.744	0.403	0.446	0.710	0.857
	Summer	-	0.971	0.535	0.014	0.676	0.285	0.682	0.667	0.568	0.913	0.846
	Fall	-	0.929	0.506	0.072	0.593	0.606	0.461	0.628	0.558	0.723	0.726
NH ₄ ⁺	Winter	-	-	0.344	0.063	0.525	0.675	0.524	0.531	0.284	0.751	0.664
	Spring	-	-	0.011	0.752	0.150	0.671	0.627	0.157	0.189	0.654	0.854
	Summer	-	-	0.376	0.055	0.527	0.144	0.555	0.506	0.382	0.827	0.743
	Fall	-	-	0.288	0.067	0.384	0.403	0.292	0.379	0.343	0.682	0.573
Cl ⁻	Winter	-	-	-	0.048	0.939	0.587	0.819	0.923	0.828	0.354	0.428
	Spring	-	-	-	0.079	0.988	0.417	0.767	0.970	0.856	0.092	0.165
	Summer	-	-	-	0.027	0.927	0.269	0.866	0.896	0.709	0.658	0.709
	Fall	-	-	-	0.254	0.880	0.554	0.505	0.927	0.606	0.288	0.442
Br ⁻	Winter	-	-	-	-	0.077	0.509	0.309	0.082	0.039	0.049	0.328
	Spring	-	-	-	-	0.162	0.842	0.829	0.205	0.139	0.247	0.824
	Summer	-	-	-	-	0.061	0.588	0.154	0.260	0.017	0.056	0.013
	Fall	-	-	-	-	0.134	0.209	0.123	0.180	0.111	0.046	0.086
Na ⁺	Winter	-	-	-	-	-	0.729	0.769	0.986	0.588	0.504	0.575
	Spring	-	-	-	-	-	0.543	0.816	0.986	0.912	0.154	0.390
	Summer	-	-	-	-	-	0.264	0.970	0.946	0.724	0.804	0.855
	Fall	-	-	-	-	-	0.655	0.596	0.971	0.697	0.393	0.618
K ⁺	Winter	-	-	-	-	-	-	0.785	0.748	0.611	0.591	0.776
	Spring	-	-	-	-	-	-	0.965	0.562	0.497	0.234	0.872
	Summer	-	-	-	-	-	-	0.155	0.505	0.798	0.290	0.281
	Fall	-	-	-	-	-	-	0.529	0.623	0.782	0.370	0.898
Ca ²⁺	Winter	-	-	-	-	-	-	-	0.795	0.997	0.433	0.564
	Spring	-	-	-	-	-	-	-	0.678	0.715	0.283	0.838
	Summer	-	-	-	-	-	-	-	0.899	0.638	0.798	0.868
	Fall	-	-	-	-	-	-	-	0.580	0.539	0.310	0.499
Mg ²⁺	Winter	-	-	-	-	-	-	-	-	0.565	0.477	0.570
	Spring	-	-	-	-	-	-	-	-	0.908	0.156	0.390
	Summer	-	-	-	-	-	-	-	-	0.851	0.779	0.826
	Fall	-	-	-	-	-	-	-	-	0.704	0.476	0.581
NO ₃ ⁻	Winter	-	-	-	-	-	-	-	-	-	0.483	0.684
	Spring	-	-	-	-	-	-	-	-	-	0.286	0.433
	Summer	-	-	-	-	-	-	-	-	-	0.658	0.689
	Fall	-	-	-	-	-	-	-	-	-	0.325	0.752
MSA ⁻	Winter	-	-	-	-	-	-	-	-	-	-	0.735
	Spring	-	-	-	-	-	-	-	-	-	-	0.454
	Summer	-	-	-	-	-	-	-	-	-	-	0.880
	Fall	-	-	-	-	-	-	-	-	-	-	0.478

Table S4: Compilation of correlation coefficient (r) values for the PM₁₀ relationships between different ion components in each season. The ion that was used on the y-axis is listed in the row and the ion it was plotted against on the x-axis is the column header. Fits that are not considered significant ($r < 0.5$) are listed in grey, highly significant fits ($r > 0.8$) are bolded.

		SO ₄ ²⁻	NH ₄ ⁺	Cl ⁻	Br ⁻	Na ⁺	K ⁺	Ca ²⁺	Mg ²⁺	NO ₃ ⁻	MSA ⁻	Oxalate
PM ₁₀	Winter	0.010	0.228	0.239	0.922	0.070	0.321	0.957	0.080	0.856	0.036	0.215
	Spring	0.196	0.360	0.031	0.031	0.040	0.132	0.012	0.057	0.143	0.254	0.750
	Summer	0.849	0.737	0.618	0.078	0.679	0.720	0.635	0.706	0.667	0.573	0.632
	Fall	0.724	0.118	0.867	0.610	0.896	0.806	0.794	0.934	0.651	0.407	0.533
SO ₄ ²⁻	Winter	-	0.367	0.841	0.078	0.834	0.848	0.054	0.824	0.136	0.271	0.368
	Spring	-	0.604	0.352	0.362	0.475	0.687	0.549	0.508	0.740	0.624	0.609
	Summer	-	0.920	0.454	0.058	0.515	0.244	0.434	0.501	0.570	0.797	0.732
	Fall	-	0.697	0.626	0.442	0.663	0.690	0.665	0.694	0.793	0.543	0.754
NH ₄ ⁺	Winter	-	-	0.081	0.182	0.012	0.085	0.099	0.040	0.279	0.075	0.634
	Spring	-	-	0.243	0.432	0.168	0.214	0.003	0.131	0.393	0.524	0.716
	Summer	-	-	0.138	0.038	0.243	0.129	0.231	0.231	0.357	0.664	0.553
	Fall	-	-	0.015	0.053	0.040	0.153	0.058	0.055	0.614	0.615	0.616
Cl ⁻	Winter	-	-	-	0.299	0.925	0.913	0.104	0.947	0.125	0.410	0.042
	Spring	-	-	-	0.060	0.851	0.662	0.826	0.921	0.209	0.118	0.026
	Summer	-	-	-	0.153	0.884	0.283	0.758	0.881	0.632	0.429	0.549
	Fall	-	-	-	0.710	0.992	0.894	0.920	0.971	0.553	0.146	0.342
Br ⁻	Winter	-	-	-	-	0.101	0.276	0.886	0.187	0.871	0.207	0.148
	Spring	-	-	-	-	0.022	0.549	0.397	0.072	0.011	0.038	0.368
	Summer	-	-	-	-	0.176	0.035	0.194	0.162	0.050	0.091	0.089
	Fall	-	-	-	-	0.710	0.657	0.627	0.747	0.331	0.238	0.227
Na ⁺	Winter	-	-	-	-	-	0.947	0.055	0.980	0.001	0.505	0.137
	Spring	-	-	-	-	-	0.725	0.827	0.916	0.410	0.060	0.143
	Summer	-	-	-	-	-	0.616	0.918	0.988	0.575	0.452	0.586
	Fall	-	-	-	-	-	0.909	0.928	0.976	0.607	0.199	0.394
K ⁺	Winter	-	-	-	-	-	-	0.128	0.926	0.187	0.377	0.292
	Spring	-	-	-	-	-	-	0.798	0.775	0.370	0.129	0.373
	Summer	-	-	-	-	-	-	0.569	0.613	0.153	0.238	0.293
	Fall	-	-	-	-	-	-	0.906	0.883	0.676	0.128	0.594
Ca ²⁺	Winter	-	-	-	-	-	-	-	0.030	0.866	0.426	0.171
	Spring	-	-	-	-	-	-	-	0.784	0.396	0.032	0.210
	Summer	-	-	-	-	-	-	-	0.894	0.372	0.389	0.551
	Fall	-	-	-	-	-	-	-	0.893	0.586	0.150	0.412
Mg ²⁺	Winter	-	-	-	-	-	-	-	-	0.027	0.565	0.063
	Spring	-	-	-	-	-	-	-	-	0.327	0.026	0.084
	Summer	-	-	-	-	-	-	-	-	0.577	0.446	0.551
	Fall	-	-	-	-	-	-	-	-	0.650	0.248	0.438
NO ₃ ⁻	Winter	-	-	-	-	-	-	-	-	-	0.067	0.419
	Spring	-	-	-	-	-	-	-	-	-	0.494	0.643
	Summer	-	-	-	-	-	-	-	-	-	0.363	0.579
	Fall	-	-	-	-	-	-	-	-	-	0.563	0.756
MSA ⁻	Winter	-	-	-	-	-	-	-	-	-	-	0.213
	Spring	-	-	-	-	-	-	-	-	-	-	0.367
	Summer	-	-	-	-	-	-	-	-	-	-	0.681
	Fall	-	-	-	-	-	-	-	-	-	-	0.491

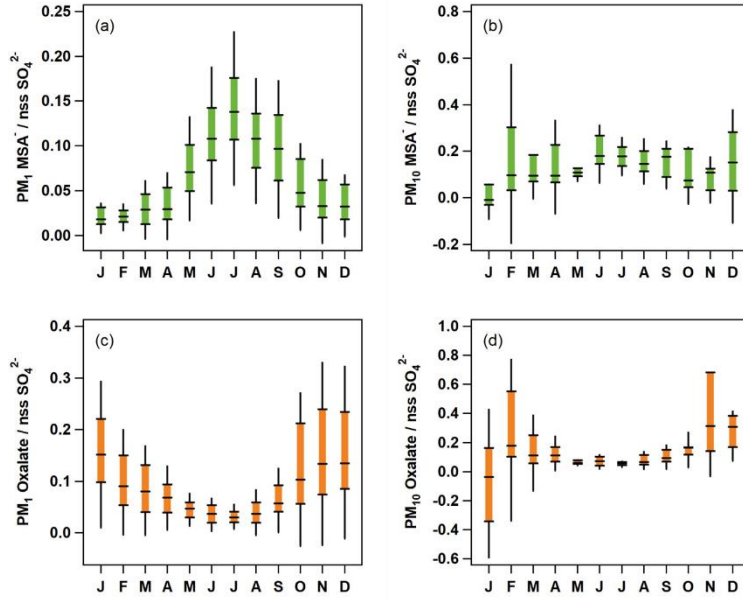


Figure S4: MSA⁻ to nss SO₄²⁻ mass concentration ratio for (a) PM₁ and (b) PM₁₀. Oxalate to nss SO₄²⁻ mass concentration ratio for (c) PM₁ and (d) PM₁₀.

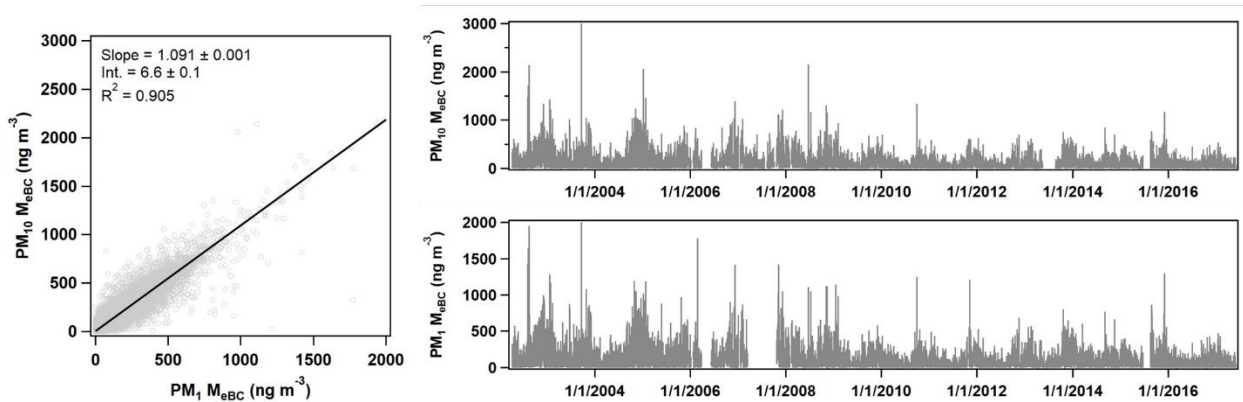


Figure S5: Calculated effective black carbon mass (M_{eBC}) for both PM10 (top right) and PM1 (bottom right). Linear relationships between PM10 and PM1 M_{eBC} indicate that the majority of M_{eBC} is in the PM1 size range.

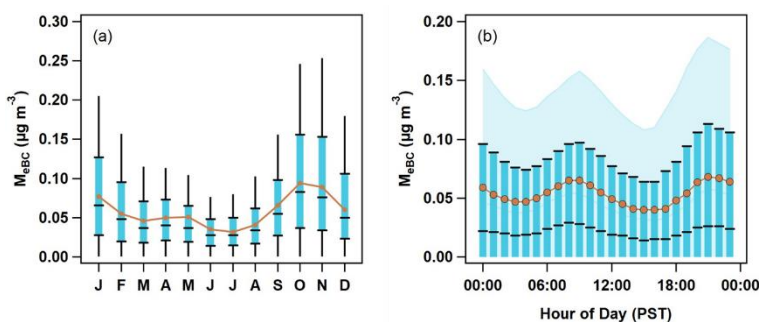


Figure S6: (a) Seasonal and (b) diurnal cycles of the calculated effective black carbon mass (M_{eBC}). Data are plotted against local time (Pacific Standard Time). The PM1 25th to 95th percentiles are indicated by black lines in (a) and blue shading in (b). The PM1 25th to 75th interval is highlighted by blue boxes and black markers. Finally, PM1 median values are black markers and PM10 median values are the orange traces.

Table S5: Compilation of correlation coefficient (r) values for the M_{eBC} PM1 relationships to different ion components in each month and each season. For both SO_4^{2-} and K^+ , the correlation coefficient is reported for both linear fit to entire ion mass and the non-sea salt (nss) fraction. Fits that are considered significant ($r > 0.5$) or are extremely close to becoming so are bolded. For ions where no or very few significant correlations to M_{eBC} were observed, data are omitted from this table.

	PM ₁	SO ₄ ²⁻	nss SO ₄ ²⁻	K ⁺	nss K ⁺	NO ₃ ⁻	MSA ⁻	Oxalate
Jan	0.419	0.523	0.524	0.567	0.569	0.334	0.322	0.538
Feb	0.128	0.148	0.299	0.068	0.184	0.003	0.156	0.324
March	0.332	0.476	0.309	0.404	0.549	-0.10	0.293	0.386
April	0.161	0.153	0.206	0.240	0.276	0.023	0.098	-0.08
May	0.116	0.176	0.130	0.296	0.381	0.067	-0.05	0.204
June	-0.02	0.077	0.092	0.098	0.168	-0.15	-0.14	0.245
July	0.349	0.210	0.173	0.439	0.514	0.234	0.302	0.270
Aug	0.418	0.154	0.134	0.573	0.475	0.239	0.266	0.511
Sep	0.268	-0.16	-0.13	0.243	0.315	0.209	-0.08	0.071
Oct	0.319	0.301	0.248	0.500	0.530	0.263	0.265	0.418
Nov	0.379	0.403	0.428	0.462	0.482	0.108	0.433	0.489
Dec	0.537	0.568	0.607	0.504	0.555	0.541	0.666	0.696
Winter	0.340	0.364	0.389	0.411	0.434	0.092	0.323	0.536
Spring	0.187	0.353	0.422	0.299	0.376	-0.02	0.203	0.213
Summer	0.281	0.175	0.161	0.330	0.417	0.136	0.204	0.348
Fall	0.339	0.040	0.050	0.393	0.376	0.196	-0.06	0.308

Table S6: Compilation of correlation coefficient (r) values for the M_{eBC} PM10 relationships to different ion components presented in Table S4 in each month and each season. For both SO_4^{2-} and K^+ , the correlation coefficient is reported for both linear fit to entire ion mass and the non-sea salt (nss) fraction. Fits that are considered significant ($r > 0.5$) or extremely close to becoming so are bolded.

	PM ₁₀	SO ₄ ²⁻	nss SO ₄ ²⁻	K ⁺	nss K ⁺	NO ₃ ⁻	MSA ⁻	Oxalate
Jan	-0.20	0.170	0.479	-0.10	0.573	0.493	0.818	0.702
Feb	-0.52	-0.52	-0.07	-0.56	0.532	-0.16	0.629	-0.19
March	-0.26	0.400	0.147	0.274	0.393	0.305	0.287	-0.04
April	-0.40	0.071	0.318	-0.11	0.134	0.401	0.006	0.189
May	0.415	-0.16	0.002	-0.26	0.372	0.129	-0.04	0.161
June	0.211	0.206	-0.14	0.710	0.503	0.308	-0.27	0.492
July	0.273	-0.11	-0.14	0.721	0.758	0.125	-0.04	0.057
Aug	-0.35	0.108	-0.23	0.307	-0.31	0.091	0.171	0.723
Sep	0.053	0.123	0.080	0.303	-0.09	0.167	-0.18	0.189
Oct	-0.53	-0.10	0.150	0.026	0.450	0.520	-0.16	0.598
Nov	0.663	0.617	0.593	0.655	0.908	0.559	0.567	0.981
Dec	0.470	0.088	0.405	0.084	0.245	0.520	0.799	0.916
Winter	-0.02	-0.11	0.282	-0.23	0.410	0.122	0.660	0.376
Spring	-0.24	0.069	0.100	-0.14	0.514	0.317	-0.04	0.003
Summer	-0.04	-0.05	-0.06	0.298	0.446	0.320	-0.21	0.317
Fall	0.279	0.220	0.020	0.445	0.667	0.281	-0.22	0.431

Section S4: Further details of PMF and error analysis

The PMF analysis of winter data resulted in a three-factor solution, while analysis on the summer data resulted in a two-factor solution (**Fig S7**). Because the seasons were run separately from each other the conditions of certain ionic species were different in the two analyses. Table S7 identifies how each ion was treated (i.e. strong, weak, or bad) for the winter and summer PMF analysis. For the winter the observed changes in Q for DISP and BS-DISP were 0.00019% and 0.019% respectively. For the summer analysis changes in Q for DISP and BS-DISP were 0.00043% and 0.05% respectively. No swaps were reported for either season and the results of the bootstrap mapping are listed in **Table S8**. Further details of error analysis methods can be found in the PMF version 5.0 user manual (Norris et al., 2014).

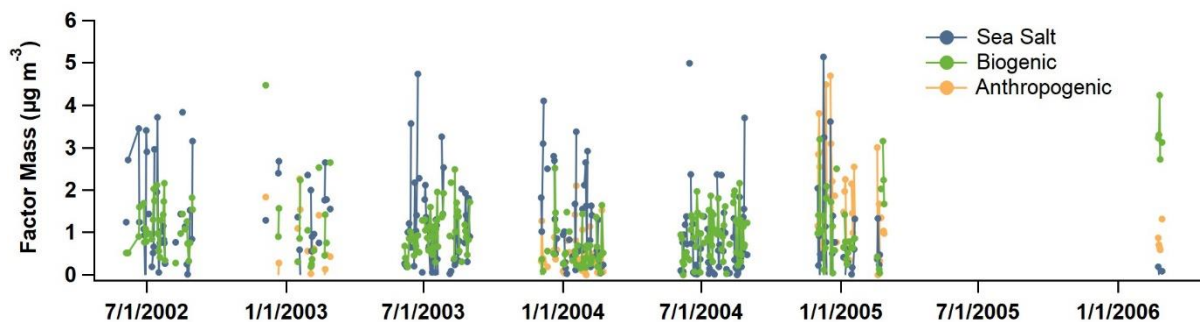


Figure S7: Timeseries of factor mass for the winter and summer PMF analysis.

Table S7: Ion treatment in the winter and summer PMF analysis. Strong ions were considered with their inputted associated error, weak ions had an additional 3% error applied, and weak ions were omitted from the PMF analysis. Classifications were determined based on signal to noise ratio (>1.0 indicated weak, and >0.5 indicated bad), as well as the predicted versus actual concentrations that resulted from an initial base run of the PMF analysis.

Ionic Species	Winter PMF	Summer PMF
Br	BAD	BAD
Na	STRONG	STRONG
Cl	STRONG	BAD
Ca	BAD	WEAK
Mg	STRONG	STRONG
SO4	STRONG	STRONG
MSA	WEAK	WEAK
NH4	STRONG	STRONG
Oxalate	STRONG	WEAK
NO3	WEAK	WEAK
K	STRONG	WEAK
eBC	WEAK	BAD

Table S8: Results from the winter and summer bootstrap mapping

Winter				
	Factor 1: Sea Salt	Factor 2: Biogenic	Factor 3: Anthropogenic / Combustion	Unmapped
Bootstrap Factor 1	100	0	0	0
Bootstrap Factor 2	0	100	0	0
Bootstrap Factor 3	0	1	99	0

Summer			
	Factor 1: Sea Salt	Factor 2: Biogenic	Unmapped
Bootstrap Factor 1	100	0	0
Bootstrap Factor 2	0	100	0

Section S5: Detailed seasonal and diurnal cycles for $f(\text{RH}=85\%)$

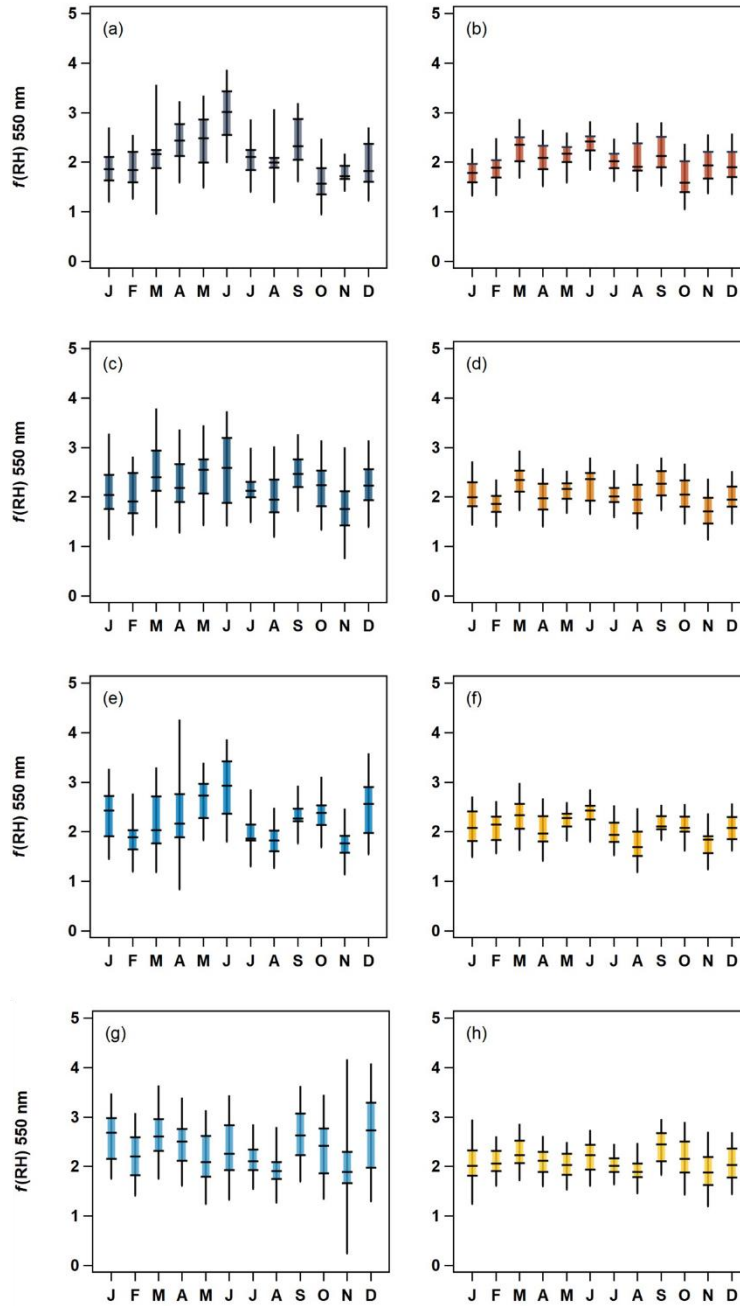


Figure S8: Seasonal cycles in PM_1 (blue, left column) and PM_{10} (orange, right column) $f(\text{RH})$ from four major wind quadrants (a, b) northeast (NE, $0 - 90^\circ$), (c, d) southeast (SE, $90 - 180^\circ$), (e, f) southwest (SW, $180 - 270^\circ$), and (g, h) northwest (NW, $270 - 360^\circ$).

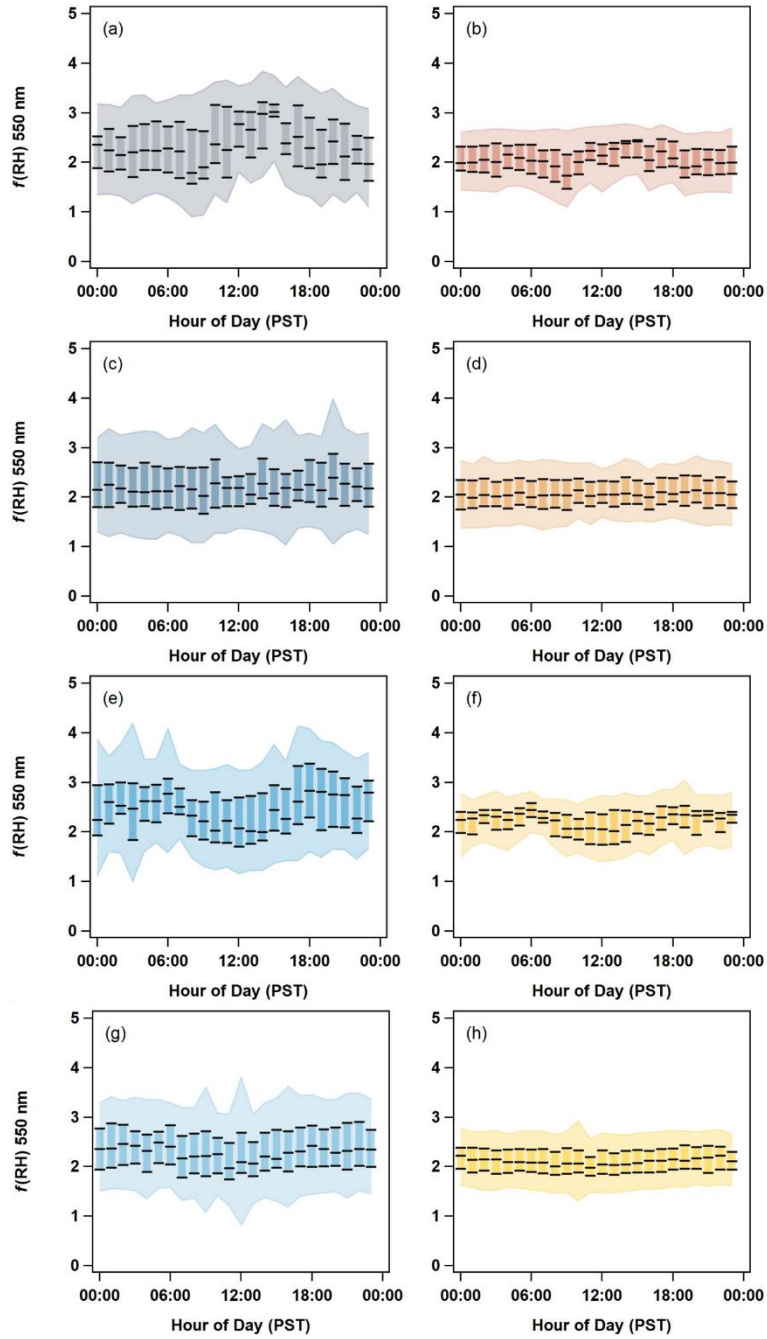


Figure S9: Diurnal cycles in PM_1 (blue, left column) and PM_{10} (orange, right column) $f(RH)$ from four major wind quadrants **(a, b)** northeast (NE, $0 - 90^\circ$), **(c, d)** southeast (SE, $90 - 180^\circ$), **(e, f)** southwest (SW, $180 - 270^\circ$), and **(g, h)** northwest (NW, $270 - 360^\circ$).

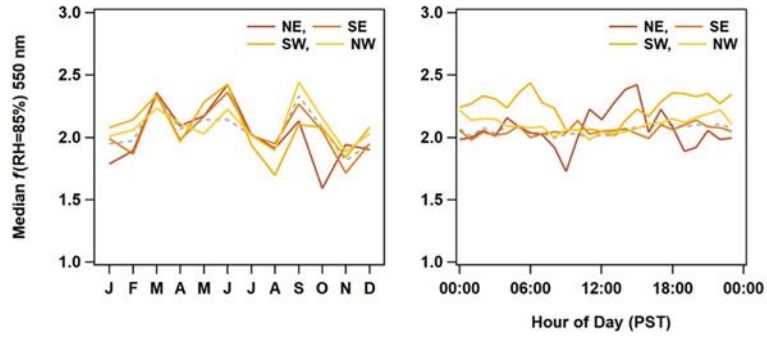


Figure S10: (left) Seasonal and (right) diurnal cycles of $PM_{10} f(RH)$. Data from each wind quadrant is represented by a different shade and trace format as outlined in the legend (northeast (NE), southeast (SE), southwest (SW), and northwest (NW)). The median for all data is represented by the grey dashed line.

Section S6: Aerosol type classification as a function of season and wind direction

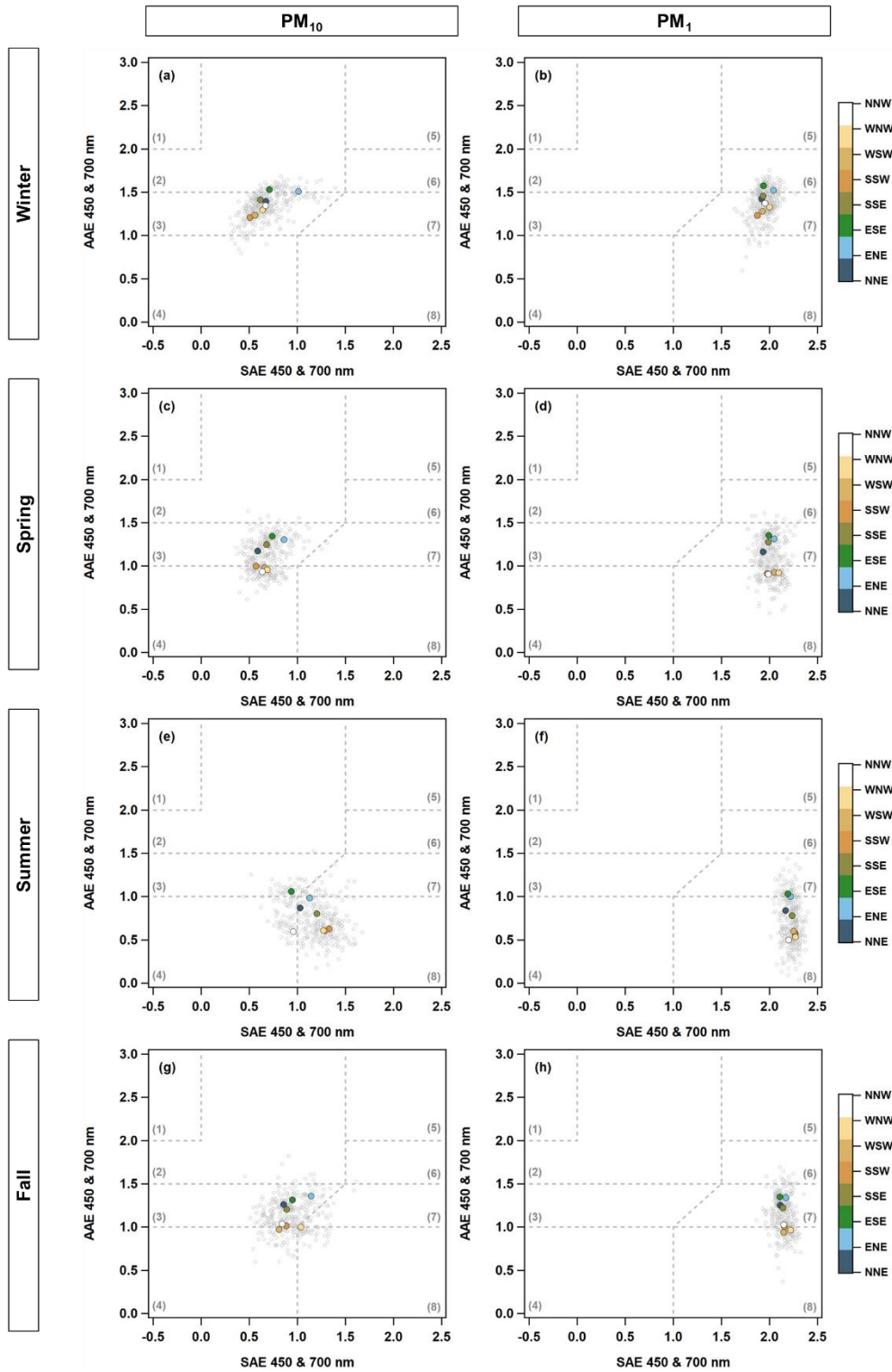


Figure S11: Wind direction dependent comparison of PM_{10} (left column) and PM_1 (right column) AAE to SAE (450 & 700 nm) in the different seasons: (a, b) winter, (c, d) spring, (e, f) summer, (g, h) fall. In each plot grey open markers represent medians at 1-degree resolution and colored markers represent median values for 45-degree resolution. A color scale is shown to indicate the wind direction represented by the colored markers: north northeast

(NNE, 0 – 45°), east northeast (ENE, 45 – 90°), east southeast (ESE, 90 – 135°), south southeast (SSE, 135 – 180°), south southwest (SSW, 180 – 225°), west southwest (WSW, 225 – 270°), west northwest (WNW, 270 – 315°), and north northwest (WSW, 315 – 360°). Different regimes defined by Cappa et al. (2016) are outlined using grey markers and are labeled one through eight: (1) dust, (2) mixed dust/ BC/ BrC, (3) large particle / BC mix, (4) large particles with low absorption, (5) BrC, (6) mixed BC/ BrC, (7) BC, and (8) small particles with low absorption. Cappa et al. (2016) also suggest that regime #4 could also represent large black particles but is changed to large particles with low absorption to account for sea salt at marine sites.

Section S7: Aerosol ion and optical properties comparison information

Table S9: PM₁ scattering to ion concentration correlation coefficients (*r*)

	PM ₁	SO ₄ ²⁻	NH ₄ ⁺	Cl ⁻	Br ⁻	Na ⁺	K ⁺	Ca ²⁺	Mg ²⁺	NO ₃ ⁻	MSA ⁻	Oxalate
Jan	0.576	0.487	0.251	0.141	0.049	0.399	0.624	0.188	0.414	0.343	0.333	0.524
Feb	0.195	0.122	0.155	-0.21	-0.03	-0.09	0.149	0.185	-0.05	-0.06	0.263	0.265
March	0.517	0.667	0.489	-0.06	0.042	0.138	0.509	0.282	0.134	0.007	0.683	0.658
April	0.451	0.453	0.491	-0.06	0.387	0.228	0.388	0.286	0.323	0.279	0.508	0.479
May	0.155	0.257	0.288	-0.04	0.069	0.053	0.341	-0.00	-0.02	0.031	0.039	0.327
June	0.572	0.295	0.188	0.274	0.078	0.323	0.365	0.508	0.321	0.058	0.231	0.404
July	0.595	0.471	0.428	0.111	-0.53	0.235	0.448	0.296	0.371	0.266	0.549	0.403
Aug	0.570	0.340	0.275	0.457	-0.14	0.372	0.466	0.497	0.418	0.247	0.543	0.568
Sept	0.379	-0.061	-0.01	0.151	0.435	0.163	0.191	0.005	0.171	0.425	0.076	0.304
Oct	0.420	0.460	0.301	0.353	-0.12	0.221	0.597	0.208	0.170	0.313	0.406	0.459
Nov	0.304	0.248	0.023	0.146	0.123	0.078	0.370	0.101	0.086	0.054	0.373	0.417
Dec	0.563	0.595	0.200	0.419	-0.30	0.586	0.389	0.562	0.471	0.502	0.492	0.564
Winter	0.551	0.456	0.068	0.113	0.023	0.329	0.513	0.299	0.314	0.230	0.435	0.535
Spring	0.371	0.519	0.428	-0.05	0.280	0.124	0.384	0.088	0.103	0.154	0.378	0.543
Summer	0.532	0.353	0.309	0.291	-0.06	0.305	0.481	0.412	0.371	0.253	0.493	0.524
Fall	0.424	0.220	0.151	0.338	-0.06	0.271	0.476	0.192	0.201	0.310	0.090	0.421

Table S10: PM₁ scattering to sea salt and nss ion concentration correlation coefficients (*r*)

	Sea Salt	nss SO ₄ ²⁻	nss K ⁺	nss Ca ²⁺	nss Mg ²⁺
Jan	0.283	0.431	0.545	0.240	0.534
Feb	-0.15	0.249	0.177	0.142	0.193
March	0.095	0.572	0.463	0.282	0.711
April	0.150	0.495	0.243	-0.05	0.696
May	0.065	0.182	0.352	0.051	-0.13
June	0.332	0.278	0.245	0.633	0.408
July	0.209	0.426	0.351	0.342	0.246
Aug	0.556	0.359	0.324	0.043	0.293
Sept	0.252	0.119	0.258	-0.15	0.012
Oct	0.378	0.345	0.574	0.172	-0.03
Nov	0.179	0.256	0.300	-0.07	0.581
Dec	0.530	0.553	0.321	0.303	0.695
Winter	0.239	0.367	0.421	0.145	0.460
Spring	0.048	0.542	0.396	-0.00	0.037
Summer	0.379	0.344	0.407	0.262	0.145
Fall	0.394	0.172	0.422	0.054	-0.00

Table S11: PM₁ absorption to ion concentration correlation coefficients (*r*)

	PM ₁	SO ₄ ²⁻	NH ₄ ⁺	Cl ⁻	Br ⁻	Na ⁺	K ⁺	Ca ²⁺	Mg ²⁺	NO ₃ ⁻	MSA ⁻	Oxalate
Jan	0.421	0.522	0.405	-0.08	0.007	0.182	0.563	0.231	0.223	0.335	0.319	0.534
Feb	0.142	0.154	0.234	-0.19	-0.33	-0.03	0.062	0.394	-0.03	0.015	0.163	0.334
March	0.329	0.457	0.387	-0.22	-0.12	-0.07	0.358	0.223	-0.06	-0.04	0.228	0.374
April	0.157	0.128	0.376	-0.30	-0.11	-0.15	0.212	0.167	-0.16	0.009	0.052	-0.12
May	0.126	0.176	0.242	-0.02	0.072	0.084	0.293	-0.08	-0.10	0.072	-0.04	0.204
June	-0.02	0.076	0.165	0.059	-0.07	-0.05	0.103	0.065	-0.04	-0.15	-0.14	0.250
July	0.358	0.213	0.281	-0.10	-0.20	-0.09	0.419	0.038	0.036	0.238	0.309	0.273
Aug	0.425	0.156	0.080	0.268	-0.09	0.227	0.571	0.318	0.294	0.236	0.264	0.516
Sept	0.271	-0.16	-0.07	-0.17	0.355	-0.08	0.244	0.071	-0.03	0.209	-0.07	0.074
Oct	0.322	0.300	0.242	0.126	-0.08	0.094	0.500	0.133	0.046	0.261	0.268	0.420
Nov	0.347	0.385	0.143	0.002	-0.12	0.011	0.401	0.197	0.003	0.145	0.433	0.489
Dec	0.489	0.484	0.208	0.017	-0.09	0.266	0.382	0.409	0.141	0.481	0.602	0.694
<hr/>												
Winter	0.369	0.368	0.145	-0.06	-0.17	0.175	0.419	0.293	0.079	0.148	0.332	0.535
Spring	0.207	0.350	0.404	-0.26	-0.08	-0.08	0.249	0.098	-0.09	-0.00	0.223	0.199
Summer	0.282	0.180	0.199	0.08	-0.05	-0.02	0.324	0.098	0.054	0.128	0.206	0.351
Fall	0.340	0.043	0.038	0.111	-0.07	0.089	0.392	0.165	0.053	0.196	-0.05	0.309

Table S12: PM₁ absorption to nss ion concentration correlation coefficients (*r*)

	Sea Salt	nss SO ₄ ²⁻	nss K ⁺	nss Ca ²⁺	nss Mg ²⁺
Jan	0.042	0.536	0.570	0.320	0.530
Feb	-0.10	0.295	0.100	0.393	0.084
March	-0.15	0.339	0.467	0.247	-0.03
April	-0.22	0.166	0.198	0.127	0.180
May	0.169	0.129	0.349	-0.08	-0.19
June	0.017	0.091	0.106	0.214	0.156
July	-0.13	0.147	0.443	0.230	0.109
Aug	0.350	0.179	0.489	-0.10	0.235
Sept	-0.06	-0.052	0.327	0.076	0.024
Oct	0.143	0.256	0.519	0.153	-0.06
Nov	0.103	0.402	0.337	-0.05	-0.306
Dec	0.173	0.518	0.408	0.396	0.940
<hr/>					
Winter	0.051	0.391	0.401	0.282	0.511
Spring	-0.21	0.410	0.295	0.176	0.139
Summer	0.141	0.186	0.408	0.040	0.019
Fall	0.176	0.018	0.369	0.062	-0.12

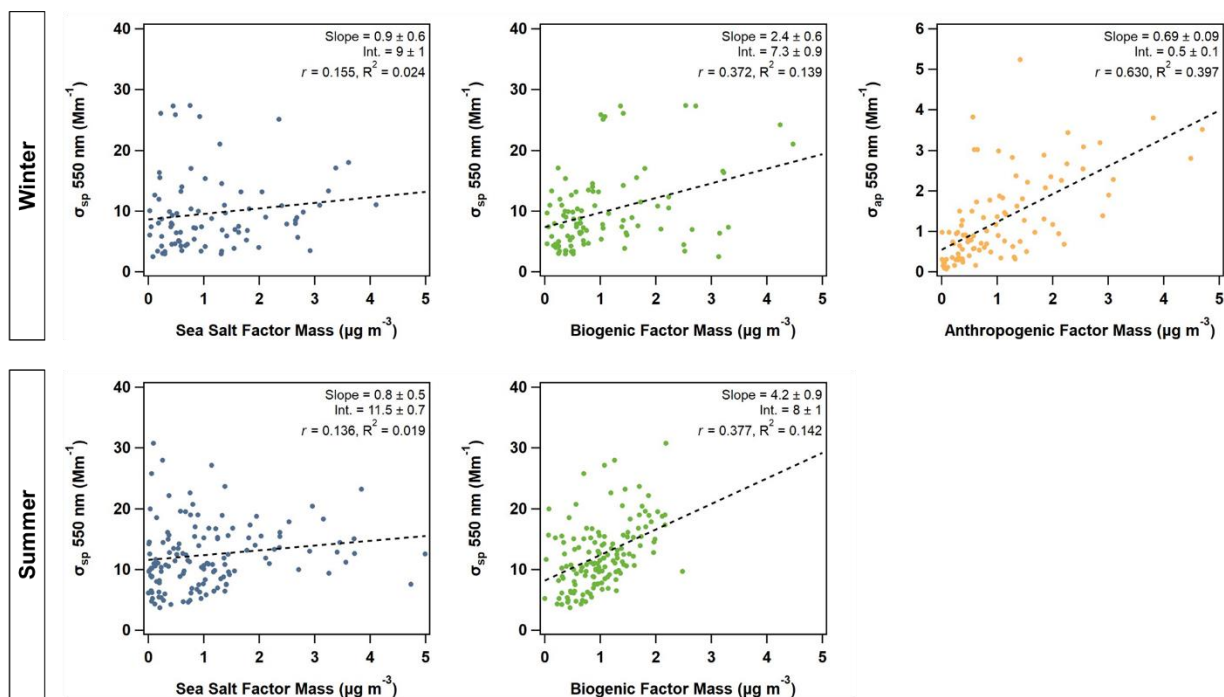


Figure S12: Scattering coefficient (σ_{sp}) compared to the sea salt and biogenic factors from the winter and summer PMF results and the absorption coefficient (σ_{ap}) compared to the anthropogenic/ combustion factor from the winter PMF analysis.

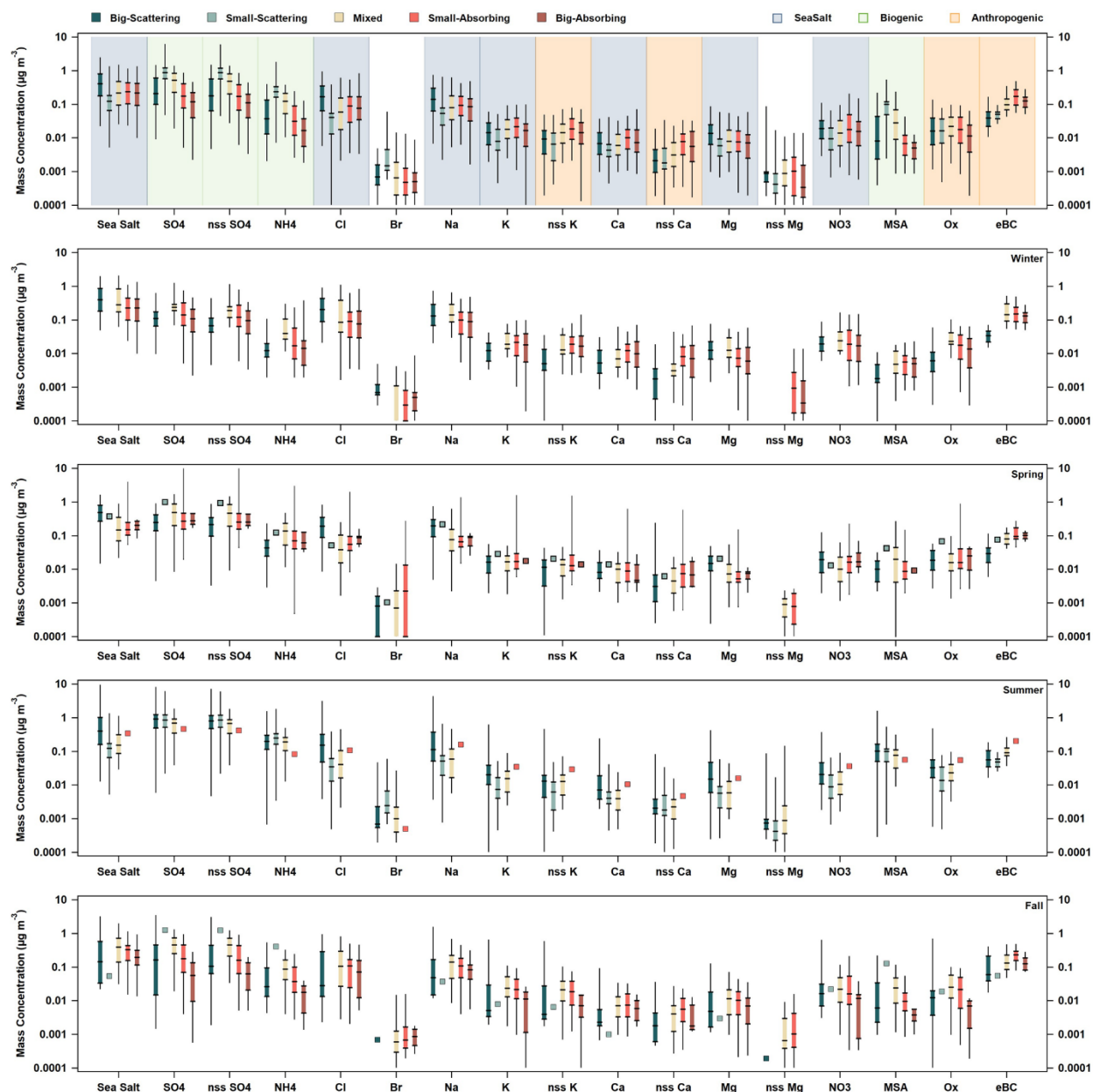


Figure S13: PM₁ ion mass concentrations, as well as sea salt and M_{eBC}, as a function of SSA (550 nm) and SAE (450 & 550 nm). For each species mass of big-scattering (SSA > 0.95, SAE < 1.91), small-scattering (SSA > 0.95, SAE > 2.24), mixed (0.89 < SSA < 0.95, 1.91 < SAE < 2.25), small-absorbing (SSA < 0.89, SAE > 2.24), and big-absorbing (SSA < 0.89, SAE < 1.91) aerosol fractions are listed from left to right and color coded as outlined in the top left legend. The top panel is Fig. 9 from the text and shows the patterns for the entire sorted data set. Subsequent panels show the grouping as a function of season (labeled in upper right of panel). In the seasonal data, missing points indicate that no data from that season fit the bounds listed above and single square markers for a group indicate that only 1 – 3 data points were available and an average is presented in place of a full statistical spectrum.

References

Cappa, C. D., Kolesar, K. R., Zhang, X., Atkinson, D. B., Pekour, M. S., Zaveri, R. A., Zelenyuk, A., and Zhang, Q.: Understanding the optical properties of ambient sub- and supermicron particulate matter: results from the CARES 2010 field study in northern California, *Atmospheric Chemistry and Physics*, 16, 6511–6535, <https://doi.org/10.5194/acp-16-6511-2016>, 2016.

Norris, G., Duvall, R., Brown, S., and Bai, S.: EPA Positive Matrix Factorization (PM F) 5.0 Fundamentals and User Guide, United States Environmental Protection Agency, Office of Research and Development, Washington DC, 2014.

Perry, K. D., Cliff, S. S., and Jimenez-Cruz, M. P.: Evidence for hygroscopic mineral dust particles from the Intercontinental Transport and Chemical Transformation Experiment, *Journal of Geophysical Research: Atmospheres*, 109, <https://doi.org/10.1029/2004JD004979>, 2004.